

Appendix 1 Formulas of radscore

Ki-67

$$\begin{aligned} \text{Radscore} = & -1.185 * \text{DWISmallAreaEmphasis} + 1.938 * \text{DWIMeanDeviation} + 0.803 * \text{DWIGreyLevelNonuniformity_} \\ & \text{AllDirection_offset4_SD} + 0.348 * \text{DWIVariance} + 0.798 * \text{DWILargeAreaEmphasis} + 0.651 * \\ & \text{DWIRunLengthNonuniformity_AllDirection_offset1_SD} + -0.727 * \text{T2Correlation_AllDirection_offset1_SD} + 0.226 \\ & * \text{T2ShortRunEmphasis_angle135_offset1} + 0.884 * \text{T2Inertia_AllDirection_offset7_SD} + -0.773 * \text{T2GLCMEntropy_} \\ & \text{AllDirection_offset7_SD} + 0 * \text{DWICorrelation_AllDirection_offset7_SD} + -0.694 * \text{T2GreyLevelNonuniformity_} \\ & \text{AllDirection_offset7_SD} + -0.925 * \text{DWILongRunEmphasis_angle0_offset4} + -0.511 * \text{T2ClusterShade_AllDirection_} \\ & \text{offset1_SD} + -0.039 * \text{DWIClusterShade_angle135_offset7} + -0.453 * \text{DWIClusterProminence_angle45_offset7} + \\ & 0.748 * \text{DWILongRunEmphasis_AllDirection_offset7_SD} + -0.146 * \text{T2LowIntensitySmallAreaEmphasis} + -0.002 * \\ & \text{DWIClusterShade_AllDirection_offset1_SD} + -0.148 * \text{DWIHaraEntroy} + -0.559 * \text{DWILongRunEmphasis_angle0_} \\ & \text{offset1} + 0.298 * \text{DWIClusterShade_angle90_offset7} + -0.408 * \text{DWIShortRunEmphasis_AllDirection_offset1_} \\ & \text{SD} + 0.497 * \text{DWIInertia_AllDirection_offset7_SD} + 0.466 * \text{T2kurtosis} + -1.919 * \text{DWIRelativeDeviation} + 0.771 * \\ & \text{DWIHighGreyLevelRunEmphasis_AllDirection_offset7_SD} + 0.335 * \text{T2MeanDeviation} + 0.593 \end{aligned}$$

P53

$$\begin{aligned} \text{Radscore} = & 0.864 * \text{DWILargeAreaEmphasis} + -0.126 * \text{DWIInverseDifferenceMoment_AllDirection_} \\ & \text{offset1_SD} + -0.744 * \text{DWICorrelation_AllDirection_offset7_SD} + 0.471 * \text{T2MeanDeviation} + 0.117 * \\ & \text{DWIShortRunLowGreyLevelEmphasis_AllDirection_offset4_SD} + -0.402 * \text{DWIGreyLevelNonuniformity_} \\ & \text{AllDirection_offset4_SD} + -0.164 * \text{T2ClusterProminence_AllDirection_offset4_SD} + -0.208 * \text{DWIClusterProminence_} \\ & \text{angle45_offset7} + 0.436 * \text{DWIMeanDeviation} + -0.11 * \text{DWIInverseDifferenceMoment_angle0_offset7} + -0.018 * \\ & \text{DWILongRunEmphasis_AllDirection_offset1_SD} + 0.128 * \text{DWIClusterShade_AllDirection_offset1_SD} + 0.033 \\ & * \text{DWIShortRunHighGreyLevelEmphasis_AllDirection_offset4_SD} + -0.405 * \text{T2InverseDifferenceMoment_} \\ & \text{AllDirection_offset7_SD} + 0.215 * \text{DWICorrelation_angle45_offset7} + -0.151 * \text{T2HighIntensityLargeAreaEmphasis} \\ & + 0.295 * \text{T2ClusterProminence_angle0_offset7} + 0.445 * \text{DWIShortRunEmphasis_angle45_offset1} + 0.252 * \\ & \text{DWIHighGreyLevelRunEmphasis_AllDirection_offset7_SD} + 0.054 * \text{DWIGLCMEntropy_angle45_offset1} + 0.376 * \\ & \text{T2skewness} + 0.155 * \text{DWIInertia_angle135_offset7} + 0.088 \end{aligned}$$

EGFR

$$\begin{aligned} \text{Radscore} = & 0.183 * \text{DWIClusterShade_angle45_offset7} + -0.282 * \text{DWIClusterProminence_angle90_offset7} + 1.808 * \\ & \text{DWIkurtosis} + 1.508 * \text{T2HaralickCorrelation_AllDirection_offset7_SD} + -0.494 * \text{DWILongRunHighGreyLevelEmphasis_} \\ & \text{AllDirection_offset4_SD} + 0.618 * \text{T2GreyLevelNonuniformity_AllDirection_offset7_SD} + -1.544 * \text{T2ClusterShade_} \\ & \text{angle0_offset7} + -0.517 * \text{DWIHaralickCorrelation_angle45_offset7} + -0.381 * \text{T2LongRunEmphasis_AllDirection_offset4_} \\ & \text{SD} + 0.108 * \text{T2GLCMEntropy_angle135_offset7} + -0.238 * \text{DWIShortRunHighGreyLevelEmphasis_AllDirection_offset7_} \\ & \text{SD} + 1.321 * \text{DWISmallAreaEmphasis} + -0.763 * \text{DWIHighGreyLevelRunEmphasis_AllDirection_offset4_SD} + 0.584 * \\ & \text{DWIhistogramEnergy} + -0.236 * \text{DWICorrelation_angle0_offset7} + 0.285 * \text{DWIShortRunEmphasis_angle90_offset7} + 0.943 \\ & * \text{DWIClusterProminence_AllDirection_offset1_SD} + 0.876 * \text{T2MinIntensity} + -0.89 * \text{DWIInverseDifferenceMoment_} \\ & \text{AllDirection_offset1_SD} + -0.243 * \text{T2Correlation_AllDirection_offset1_SD} + 1.101 * \text{DWIHaralickCorrelation_} \\ & \text{angle135_offset7} + -0.75 * \text{DWIMeanDeviation} + 0.866 * \text{DWIShortRunEmphasis_angle90_offset4} + -0.027 * \\ & \text{DWILongRunEmphasis_AllDirection_offset4_SD} + -0.022 * \text{T2LargeAreaEmphasis} + 0.282 \end{aligned}$$

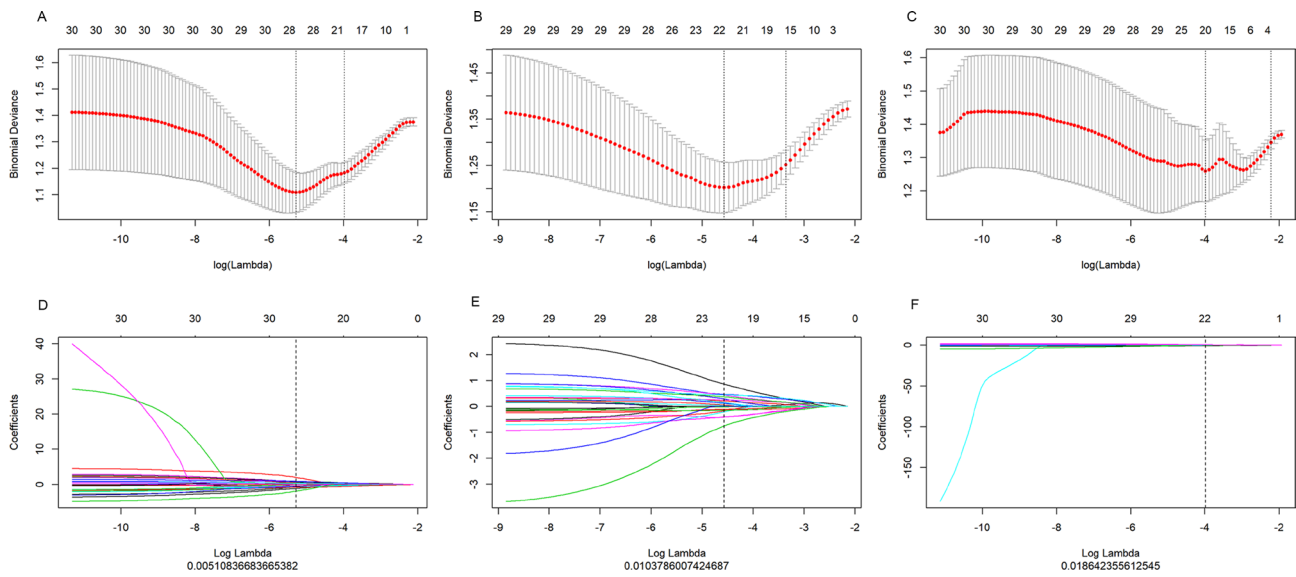


Figure S1 The LASSO procedure entailed selecting a regularization parameter λ and identifying the number of the features for Ki-67, p53, and EGFR. (A,D) Ki-67. (B,E) p53. (C,F) and EGFR.